

Preparation of Versatile, Porous Poly-Arylthioethers by Reversible Pd-Catalysed C–S/C–S Metathesis

Miguel A. Rivero-Crespo, Georgios Toupalas and Bill Morandi*

ETH Zürich, Vladimir-Prelog-Weg 1-5/10, 8093 Zürich, Switzerland

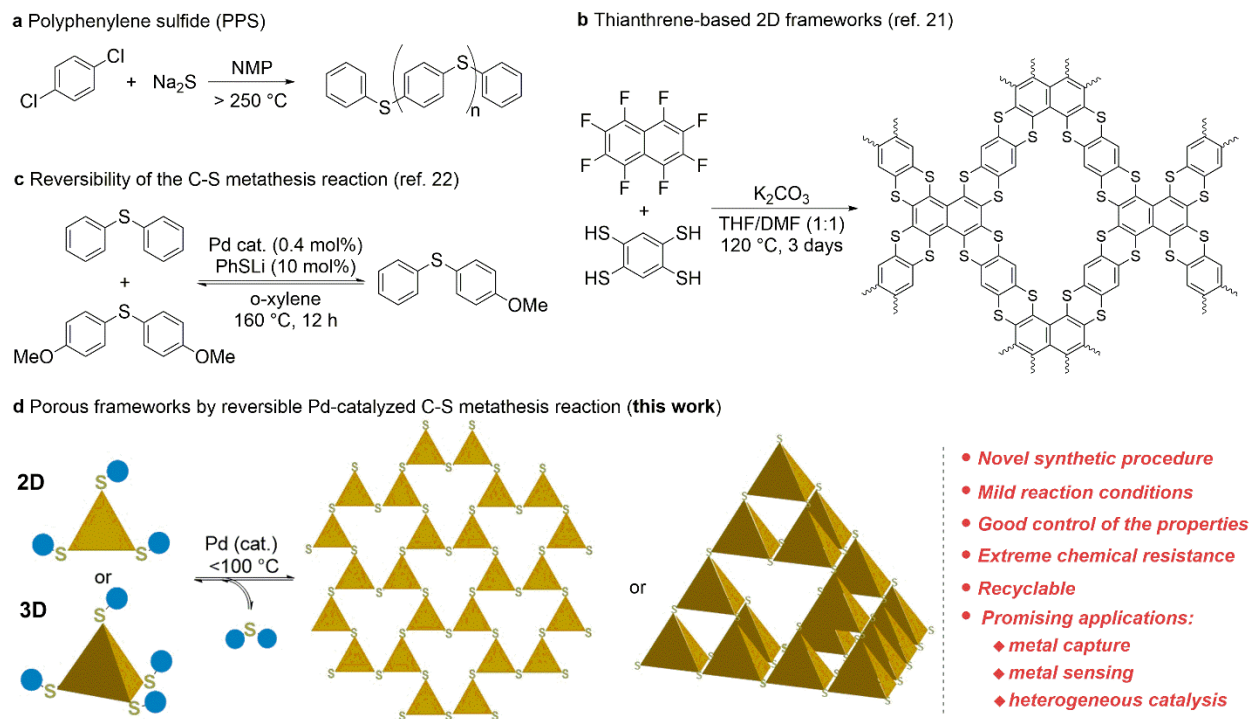
porous frameworks, homogeneous catalysis, metathesis, polymer chemistry, metal capture, metal sensing

ABSTRACT: Porous organic frameworks have shown a number of promising properties; however, their industrial application is usually hampered due to the lability of their linkages (imine, boroxine, etc.). Inspired by the outstanding chemical, mechanical and thermal resistance of the 1D polymer polyphenylene sulfide (PPS), we hypothesized that 2D and 3D poly-arylthioether frameworks would merge the attractive features common to porous frameworks and PPS in a single material. Herein, we report a Pd-catalysed C–S/C–S metathesis-based method to prepare new porous poly-arylthioether frameworks in good yields. The self-correcting nature of the process has enabled the synthesis of new, robust materials with high surface areas. Despite the frameworks' extreme resistance to harsh chemicals, they can be fully recycled to recover the original building blocks using the same catalytic reaction. In addition, we demonstrate preliminary results showing that these materials have great potential in several environmentally relevant applications including metal capture, metal sensing and heterogeneous catalysis. In a broader context, these results clearly demonstrate the untapped potential of emerging single-bond metathesis reactions in the preparation of new materials.

INTRODUCTION

Porous organic frameworks, including COFs and polymers, are a privileged class of materials with high surface area, low mass density, and modular topology that have gathered a lot of attention among the chemistry and materials science communities during the last two decades.¹⁻⁹ They have shown promising applications spanning areas from gas and metal capture, to optoelectronics and catalysis, among others.¹⁰⁻¹⁴ Dynamic covalent chemistry (DCC)¹⁵ is a key feature in the synthesis of these systems; the reversibility of the reactions used for their syntheses provides self-correcting behaviour which, in turn, allows the formation of high-quality, low-defect

materials. Despite their interesting properties, the lability of most of the linkages (e.g. imine, boronate ester, boroxine) used to construct these materials under self-correcting conditions makes them unstable towards moderately harsh media (e.g. water, pH, temperature, pressure), often hampering their industrial application. For this reason, the synthesis of analogous yet more stable materials containing stronger covalent bonds is highly attractive, especially if those bonds can be formed reversibly in a DCC-like manner. Sulphur containing 1D-polymers like polyphenylene sulphide (PPS) have seen widespread use in industry as insulators and replacements for metal parts due to their extremely high chemical, thermal and mechanical resistance, as illustrated by the large number of patents (>100'000) in this area.^{16,17} However, the harsh synthetic conditions required for their synthesis (Scheme 1a, polycondensation > 250 °C, Na₂S, autogenous pressure)^{16,18} and the extreme stability of the thioether bonds formed, make it difficult to fine-tune PPS's properties (M_w, cross-linking, polydispersity, etc.). Moreover, this synthetic method dramatically limits the possibility to access more complex poly-arylthioether-based structures with 2D or 3D cores, despite their potential to exhibit advanced features such as porosity, metal-binding sites or optoelectronic properties, among others. The synthesis of such advanced materials, which should be analogous to PPS in terms of chemical, thermal and mechanical stability, would be a step towards the industrial application of porous frameworks. Among the extremely scarce examples of porous poly-arylthioether-based materials,^{19,20} Swager and co-workers reported the synthesis of thianthrene-based 2D frameworks with high surface area and interesting redox properties using dynamic S_NAr reactions of thiocatechols and perfluorinated aromatic compounds (Scheme 1b).²¹ While this synthetic method provides an exciting new approach, it is limited to specific monomers (1,2,4,5-benzenetetrathiol with hexafluorobenzene or octafluoronaphtalene) that can participate in the S_NAr reaction. Moreover, potential applications of these materials have not yet been extensively explored. Therefore, there is a critical need to develop new, complementary approaches to fully harness the potential of porous poly-arylthioether frameworks in advanced materials and catalytic applications.



Scheme 1. Synthesis and structure for **a** PPS and **b** thianthrene-based 2D frameworks. **c** Experiment showing the reversibility of the C–S/C–S metathesis reaction: equilibrium is reached starting from both sides. **d** Approach followed in this work.

In 2017, our group reported the Pd-catalysed C–S/C–S single-bond metathesis reaction²² and, more recently, a Ni-catalysed version.²³ These reactions allow the facile synthesis of a number of thioether molecules and macrocycles from the corresponding thiols as nucleophiles and aryl–SR (R = H, Me) compounds as electrophiles by driving the equilibrium towards product formation (excess of nucleophile and precipitation of LiSMc or Li₂S salts). Interestingly, depolymerisation of PPS was achieved in 85% yield, showing the potential of the reaction for materials science.²² In addition, full reversibility was demonstrated at high temperatures (160 °C) by scrambling of the aryl groups giving a statistical mixture of products both in the forward and reverse reactions (Scheme 1c). As mentioned previously, full reversibility of the reaction is highly desirable for materials synthesis in order to obtain high quality polymers with fine-tuned properties. While transition metal catalysis is widely applied to make conventional 1D polymers, including reversible reactions such as olefin metathesis,^{24,25} their use in the synthesis of 2D and 3D porous polymers is much less developed. Some remarkable examples include the report from Dichtel and co-workers using catalytic amounts of metal triflates to make imine-COFs,²⁶ or the use of alkyne metathesis by Zhang and co-workers^{15,27,28}. For all these reasons, we decided to harness the potential of the reversible Pd-catalysed C–S/C–S metathesis reaction to synthesise 2D and 3D-frameworks. Herein, we report the synthesis of a new family of arylthioether-based porous-frameworks from simple building blocks

enabled by a fully reversible version of the Pd-catalysed C–S/C–S metathesis reaction with exquisite control over their physical properties (Scheme 1d). Moreover, the materials can be recycled to the monomers and reveal promising applications in metal capture, metal sensing and heterogeneous catalysis.

RESULTS AND DISCUSSION

Preliminary kinetic study. Translating a catalytic reaction from small molecule synthesis to materials preparation is a daunting task encompassing many challenges, such as catalyst deactivation and insufficient self-correcting ability due to unfavourable kinetics. In this context, our previous work showing one example of the fully reversible C–S/C–S metathesis of diarylthioethers at high temperatures (160 °C) needed careful re-evaluation.²² Under such harsh conditions, side reactions and catalyst decomposition become problematic and can hamper the synthesis of the materials. In order to address these issues, we studied the effect of the electronic properties on the reaction rate by performing a 2D-Hammett analysis using various symmetric arylthioethers with different substituents. Interestingly, the reaction is extremely fast, even at much lower temperatures than previously reported (80 vs. 160 °C), in a small, optimal range of matching electronic properties (Figure 1a and S1, $-0.2 < \sigma(\text{Ar}_1 \text{ and } \text{Ar}_2) < 0.2$). This observation can likely be explained by the necessity to have similar rates of oxidative addition for both substrates to facilitate a productive cross-metathesis event. We can thus conclude that the design of the optimal building blocks should rely on electronically neutral, minimally biased aromatic monomers. Noteworthy, the C–S/C–S metathesis reaction rate is in the same order of magnitude as imine condensation used for COFs synthesis (70 °C, 3.0 vs. 10.0 mM·min⁻¹, respectively, Figure S2),²⁹ which further supports the potential of this reaction in the synthesis of materials following a DCC approach. We also evaluated the effect of different parameters on the rate and catalyst lifetime in order to find the optimal range of conditions for the reaction. Temperature had a big influence on catalyst stability: the catalyst does not show significant deactivation up to 100 °C but deactivates readily at higher temperatures (Figure 1b). In general, the reaction rate is enhanced by higher catalyst and base loadings and in apolar solvents (toluene, xylenes, diphenyl ether, etc.), whereas polar aprotic or halogen-containing solvents are not compatible with the reaction (see Table S1 and Figure S3).

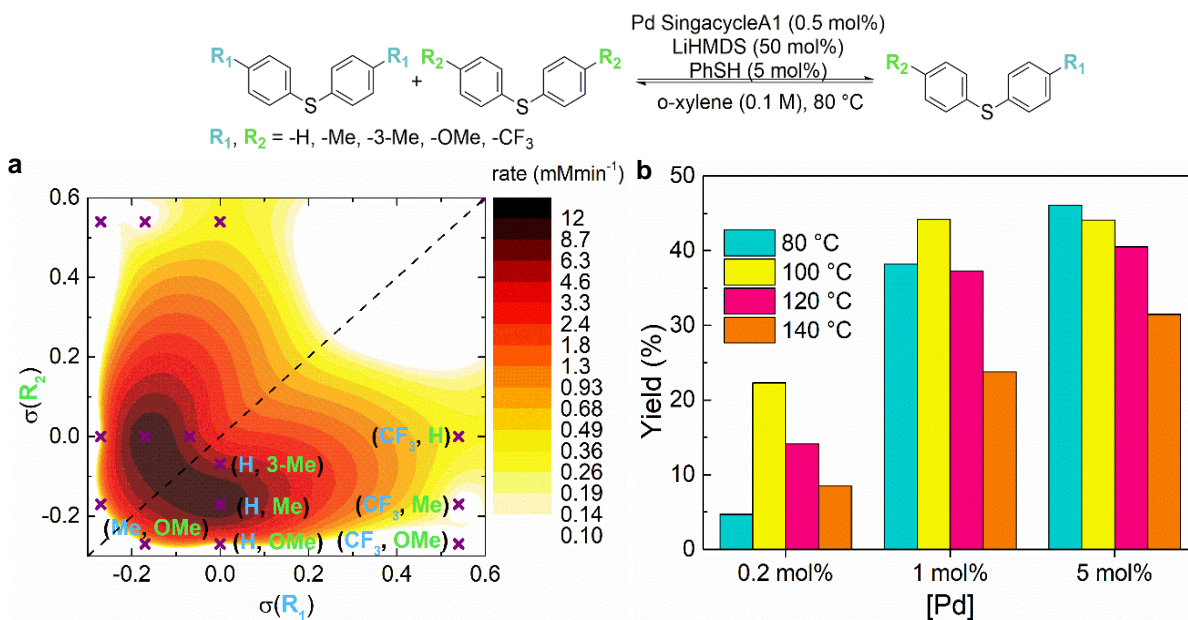


Figure 1. Preliminary mechanistic studies. **a** Kinetics of C–S/C–S metathesis (top) in the scrambling of aryl groups with different electronic properties. Note the logarithmic scale for the contour plot. **b** Yield for the model reaction (benzyl phenyl sulfide + 3-trifluoromethyl thioanisole) after 16 hours as a function of [Pd] and reaction temperature.

Design and synthesis of starting materials. Using the information gathered from the preliminary kinetic experiments, we designed the monomers containing an electronically neutral aromatic core bearing 3 or 4 phenylthioether functional groups. Seven new monomers have been synthesised by well established procedures (Figure 2a). Cores with D_{3h} (**1**, **2** and **3**), D_{2h} (**4** and **5**) and T_d (**6** and **7**) symmetry were prepared to obtain porous frameworks with diverse 2D and 3D geometries.

Synthesis and characterization of the polymers. The optimal polymerisation conditions for every monomer **1-7** were found by performing a screening within the narrow set of conditions obtained from the preliminary kinetic study ([**1-7**], [PhSH], [LiHMDS], [Pd], T, solvent and stirring, see Tables S2-S8 for details on each case). The choice of the solvent system is extremely important in the synthesis of porous polymeric structures: stabilisation of oligomers and formation of colloids in the solution during the first stages of the reaction is proposed to prevent a premature precipitation of the particles, ensuring the continuous growth and self-correction which lead to low-defect materials.³⁰ We decided to use Ph₂O as co-solvent due to its ability to partially solubilize PPS³¹ (other potential co-solvents such as NMP or PhCN unfortunately stopped the reaction presumably due to their ability to coordinate³² and reduce³³ Pd, Figure S4). Indeed, when a one-to-one mixture of *o*-xylene/Ph₂O was used as solvent system, **P1** was obtained as a colloidal suspension after 20 hours, in contrast to pure *o*-xylene that **P1**

formed a precipitate, confirming the stabilising effect of Ph₂O (in both cases, turbidity appeared after 20 minutes). Field emission scanning electron microscopy (FESEM) showed a remarkable difference in **P1** particle size for both solvent systems (50 vs. 200 nm, for *o*-xylene/Ph₂O and *o*-xylene, respectively, Figures S35 and S42). Moreover, the surface area of **P1** synthesized in pure *o*-xylene was considerably lower; from 192 for *o*-xylene/Ph₂O to 66 m²·g⁻¹ for *o*-xylene (Figures S27 and S28). Temperature had also a big impact on the particle size even in an *o*-xylene/Ph₂O mixture (50 vs. 500 nm for 80 and 120 °C, respectively, Figures S35 and S43). Thus, by modification of the temperature and the solvent system, we were able to achieve exquisite control over the particle size of the frameworks. On the other hand, other factors such as concentration or catalyst amount do not significantly influence the particle size. Pd-K edge extended X-ray absorption fine structure (EXAFS) measurements of the materials synthesised employing different reaction conditions showed that the remaining metal embedded within the framework is coordinated to sulphur (R = 1.8 Å) and carbon (R = 1.4 Å) atoms, which most likely corresponds to the oxidative addition product of the Pd into the Ar–S bond (Figures S64 and S65). This observation points towards the oxidative addition complex being the resting state of this catalytic reaction.

With the optimised conditions in hand for each building block, we performed the gram-scale synthesis of **P1-P7**. To our delight, all the materials were obtained in moderate to excellent yields (59-95% in weight), in good agreement with the conversion measured as yield of by-product (Ph₂S) by GC analysis (Table S9). As expected, controls performed without Pd catalyst or base gave neither solid formation nor conversion. These results are remarkable, as there are extremely few examples of reversible, metal-catalysed syntheses of porous materials in the literature.^{15,26-28} Notably, high surface areas were obtained in most cases (up to 526 m²·g⁻¹ for **P6**), with pore sizes in the micro/mesoporous range between 1-4 nm (Figure S27-34), which illustrates that, indeed, the frameworks maintain a porous structure, indicative of long-range ordering. In addition, FT-IR shows the disappearance of the bands associated with the pendant –SPh groups of the monomers (see Figures S17-S23), a result consistent with the yields obtained by both GC and weight.

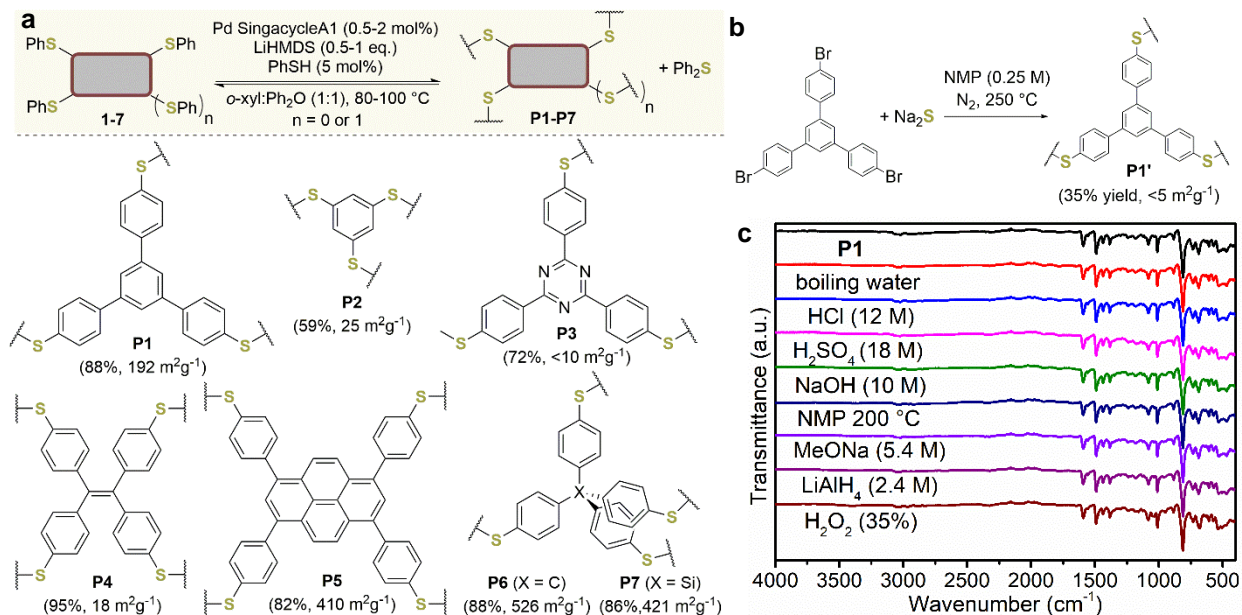


Figure 2. **a** Poly-aryltioethers synthesised from monomers 1-7. Values in parentheses show yield by mass and surface area of the polymers **P1-7**, respectively. **b** Synthesis of **P1'** via non-reversible polycondensation reaction. **c** FT-IR spectra of **P1** after 24 hours in contact with different chemicals.

A combination of different techniques was next used to investigate the properties of the materials. Elemental analysis matched the theoretical amounts of C, H, N and S for the synthesised structures (Table S10). Moreover, the Pd amount on the as-synthesised materials measured by ICP-OES oscillated in the range of 0.18-1.65 wt% (Table S11). This Pd amount can be further reduced to 0.15-0.66 wt% by washing the solid with a chelating agent (1,3-propanodiamine).³⁴ The Pd remaining in the structure is likely to be trapped in closed pores and stay inaccessible to the chelating agent under such conditions. The particle size of the polymers was in the range of 20-100 nm as determined by electron microscopy techniques (SEM and TEM, Figures S35-S43 and S53-S63). UV-vis spectroscopy showed that most materials absorb light in the UV region, whereas fluorophore-based frameworks **P4** and **P5** absorb visible light (Figure S26). More interestingly, all materials except **P2** showed fluorescence after washing (Figure 3c), particularly **P4** and **P5**, as expected from the fluorophore-based repeating units.

To demonstrate the importance of the reaction's reversibility for the synthesis of the materials, we tried to synthesise the material **P1** by the most common procedure to prepare sulphur-based polymers: polycondensation reaction of aryl halides with Na₂S at elevated temperatures (250 °C). The material **P1'** was indeed obtained according to the FT-IR spectra (Figure S24), albeit in considerably lower yield than **P1** (35% vs.

88%) and, more importantly, **P1'** was non-porous ($<5 \text{ m}^2 \cdot \text{g}^{-1}$ vs $192 \text{ m}^2 \cdot \text{g}^{-1}$ for **P1**), indicative of an amorphous, interlinked polymer formed under complete kinetic control. Particle size for **P1'** measured by FE-SEM was around $0.5 \mu\text{m}$ (Figure S44). These results highlight that while the use of standard polycondensation reactions also enables the formation of the same bonds to form similar structures, the reversibility of C–S/C–S metathesis is a crucial factor in the synthesis of these materials. This is evidenced by the significant long-range ordering through self-correction which thus results in highly porous polymers with well-defined particle sizes, a feature which is fundamental for their applications.

Chemical resistance of the framework **P1** was tested by immersion in different solutions for 24 hours: boiling water, NMP at $200 \text{ }^\circ\text{C}$, strong acids, bases, reducing agents and oxidizing agents and the FT-IR spectra before and after exposing the materials to these conditions were compared (Figure 2c). Very small differences were observed between the spectra (see Figure S25 for subtracted spectra), demonstrating the extremely high stability of the materials against harsh chemicals and conditions, similar to polyarylether-based COFs.³⁵ Remarkably and despite its stability towards harsh chemical reagents, the polymer **P1** could be recycled back to the monomers in 73% yield by reacting it under C–S/C–S metathesis conditions at $140 \text{ }^\circ\text{C}$ using an excess of cyclohexanethiol (Table S12). Interestingly, controls with no added catalyst still gave back the monomer, albeit in slightly lower yields. This might be explained by the remaining Pd embedded in the structure, that becomes accessible under these forcing conditions. This demonstrates how, in the context of sustainability, materials can be designed to be extremely stable and, at the same time, be easily decomposed back to the monomers.

Application of the frameworks to noble metal capture. Water contamination by noble metal cations is an environmental challenge due to its harmful effects on human health and ecosystems.³⁶ In addition to that, efficient recovery of expensive metals like Pd, Au and Pt from industrial waste waters can have a huge economic impact due to their scarcity and high price. The use of solids to capture metals from solutions is particularly significant in terms of reusability, especially if the metals can be easily desorbed. Several porous materials have already been used for this purpose including MOFs,³⁷ COFs³⁸ and polymers³⁹. Commonly, thiol pendant groups are anchored to the structure in a post-synthetic modification step in order to adsorb higher amounts of metals, increasing the complexity of the process. In addition, strong metal-thiol bonds make it difficult to recover the metals from the solid without damaging the structure. In our frameworks, the structural thioether groups can be directly used to adsorb precious metals reversibly without requiring further modifications, which makes the process simple and efficient. We evaluated the adsorption capacity of **P1-7** for Au^{3+} and Pd^{2+} capture, two

common and valuable pollutants in industrial wastewaters (Figure 3a). In the case of palladium, the materials were able to capture up to $69 \text{ mg}\cdot\text{g}^{-1}$ of Pd^{2+} from a 100 ppm PdCl_2 solution, which could be increased to $115 \text{ mg}\cdot\text{g}^{-1}$ starting from a 500 ppm PdCl_2 solution (Table S13). The amount of Au captured by the frameworks from a 500 ppm AuCl_3 aqueous solution was up to $295 \text{ mg}\cdot\text{g}^{-1}$ which corresponds to almost 50% of sulphur atoms in the frameworks coordinated to Au. The framework **P4** showed the highest capacity for Pd^{2+} and **P5** for Au^{3+} . ICP-OES analysis of the solids after metal capture gave slightly lower values than the calculated metal removed from the solution (10-20% lower, Table S11) which probably corresponds to some metal cations being weakly adsorbed on the surface of the solids and are removed by just washing with water. Interestingly, most of the metal cations could be easily removed from the solid by washing with 1,3-diaminopropane in NMP and the solids could be reused almost to 100% capacity over three cycles (Figure S7).

High-resolution transmission electron microscopy (HR-TEM) and high-angle annular dark-field (HAADF) coupled to EDX images show the good dispersion of the metals in the material after capture (Figure 3b). Pd-K edge EXAFS measurements indicate that the palladium is adsorbed directly on the sulphur sites ($R = 1.8 \text{ \AA}$) with different degrees of hydration⁴⁰ ($R = 1.5 \text{ \AA}$, Figures 4d and S66). Residual thiols in the frameworks can be excluded as adsorption sites since different amounts of PhSH in the synthesis of **P1** did not affect its Pd^{2+} adsorption capacity (69.3 , 69.0 and $72.3 \text{ mg}\cdot\text{g}^{-1}$ respectively for 2, 5 and 10 mol% of PhSH), pointing towards structural thioethers as binding sites.

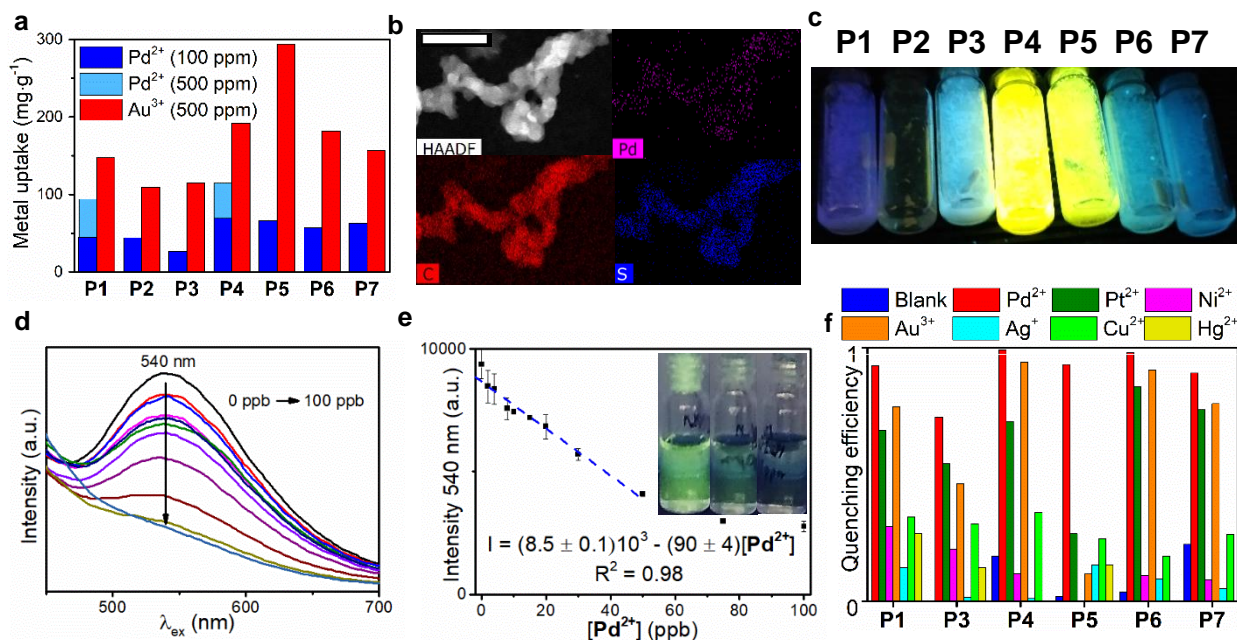


Figure 3. **a** Pd²⁺ and Au³⁺ uptake capacity for the frameworks from PdCl₂ (100 or 500 ppm) and AuCl₃ (500 ppm) aqueous solutions. **b** HAADF image and EDX mapping of Pd²⁺@P1 (1 wt%, bar represents 200 nm). **c** Fluorescence of the frameworks under 366 nm irradiation. **d** Fluorescence emission spectra ($\lambda_{\text{ex}} = 370 \text{ nm}$) of P4 in water (2 ppm) after contact with different concentrations of Pd²⁺ (from 0 to 100 ppb). **e** Fluorescence emission at the maximum (540 nm) vs. [Pd²⁺]. Inset shows the quenching of fluorescence in a dispersion of P4 (10 ppm) after adding Pd²⁺ (from left to right 0, 0.1 and 1.0 ppm). **f** Fluorescence quenching of the frameworks (50 ppm) by different metal cations (10 ppm).

Pd²⁺ sensing by coordination-induced fluorescent quenching. Metal ion sensing by fluorescence quenching is one of the methods of choice to detect metal cations in aqueous solutions due to its high sensitivity.⁴¹⁻⁴³ However, despite the suitability of using solid materials that can be easily separated from the solution and even reused, mainly small molecules have been reported for Pd²⁺ detection by fluorescent quenching. Among the few solids reported for this application, a polymer containing 2,6-bis(2-thienyl)pyridine moieties⁴⁴ and the MOF KFUPM-3⁴⁵ were shown to detect down to 400 and 44 ppb of Pd²⁺, respectively. Excitingly, the framework P4 was extremely sensitive for Pd²⁺ detection, being able to sense down to 2 ppb or 0.019 μM (Figure 3d and e). These values are comparable to the best sensors reported thus far.⁴¹⁻⁴⁵ Moreover, the response was fast (within seconds) and all the materials were extremely selective for Pd²⁺, especially P5. Indeed, the fluorescence was not affected by Cu²⁺, Ni²⁺, Ag⁺ or Hg²⁺ (Figures 3f, S8-S13) and just slightly by Au³⁺ and Pt²⁺ demonstrating the great potential of the frameworks as selective sensors for Pd²⁺ traces in water.

Catalytic application of Pd@P1. Given the high capacity of the frameworks to adsorb and disperse noble metals, preventing agglomeration, we decided to explore the capability of the hybrid material Pd²⁺@P1 (1 wt% Pd) as heterogeneous catalyst. One of the key features of a good catalyst support is the ability to stabilize metals without binding too strongly and thus reducing catalytic activity. Considering the characteristics of our new frameworks: high surface area, good dispersion of the metals and weak and reversible binding to the metal cations; we hypothesized that they could be used as supports for noble metal sites. Similar materials including carbon nitride^{46,47} or even PPS⁴⁸ have been used as supports^{46,47} to stabilize and modify catalytic activity of Pd in catalysis. Gratifyingly, Pd²⁺@P1 showed good catalytic activity for classical Pd-catalysed reactions, i.e. Suzuki-Miyaura coupling and the industrially relevant semi-hydrogenation of terminal alkynes (Figure 4a).⁴⁹ Notably, Pd²⁺@P1 could perform the semi-hydrogenation of phenylacetylene to styrene under mild conditions with high selectivity (>95%) and can be reused over 6 cycles (TON = 5860) without significant loss of activity (Figure 4b). Moreover, the hot-filtration test showed that the Suzuki and semihydrogenation reactions stopped when the solid

was filtered from the solution (Figure S14 and S16), indicating that the reaction most likely takes place at the solid/liquid interface and not in the solution due to leaching of metal species. Controls without catalyst or using the as-synthesised and the washed materials did not give any activity, confirming that the Pd remaining in the structure (analysed by ICP-OES) is not accessible to the reagents under the reaction conditions. HR-TEM and EXAFS after the Suzuki and hydrogenation reactions show that the support is able to prevent agglomeration of Pd, and only small amounts of subnanometer Pd clusters were detected (Figure 4c).

Moreover, we tested **P1** and **P6** as supports for single atom catalysts (SACs) in gas-phase reactions. Pd-K EXAFS in-situ measurements of Pd²⁺@**P1** and Pd²⁺@**P6** suggested that the materials were able to stabilize and isolate the Pd atoms preventing agglomeration even up to 300 °C under H₂ atmosphere (Figure 4d) – only a small Pd-Pd contribution appears for **P1**, whereas no Pd–Pd feature appears for **P6**, consistent with the higher surface area of the latter. X-ray absorption near edge structure (XANES) region indicate reduction of the Pd already at 100 °C (Figure S67 and S68).⁵⁰ These results confirm the potential of the sulphur-containing porous polymers as supports for gas-phase heterogeneous catalysts. Further reactivity tests are underway in our laboratories to unlock the full potential of this new family of materials in catalysis.

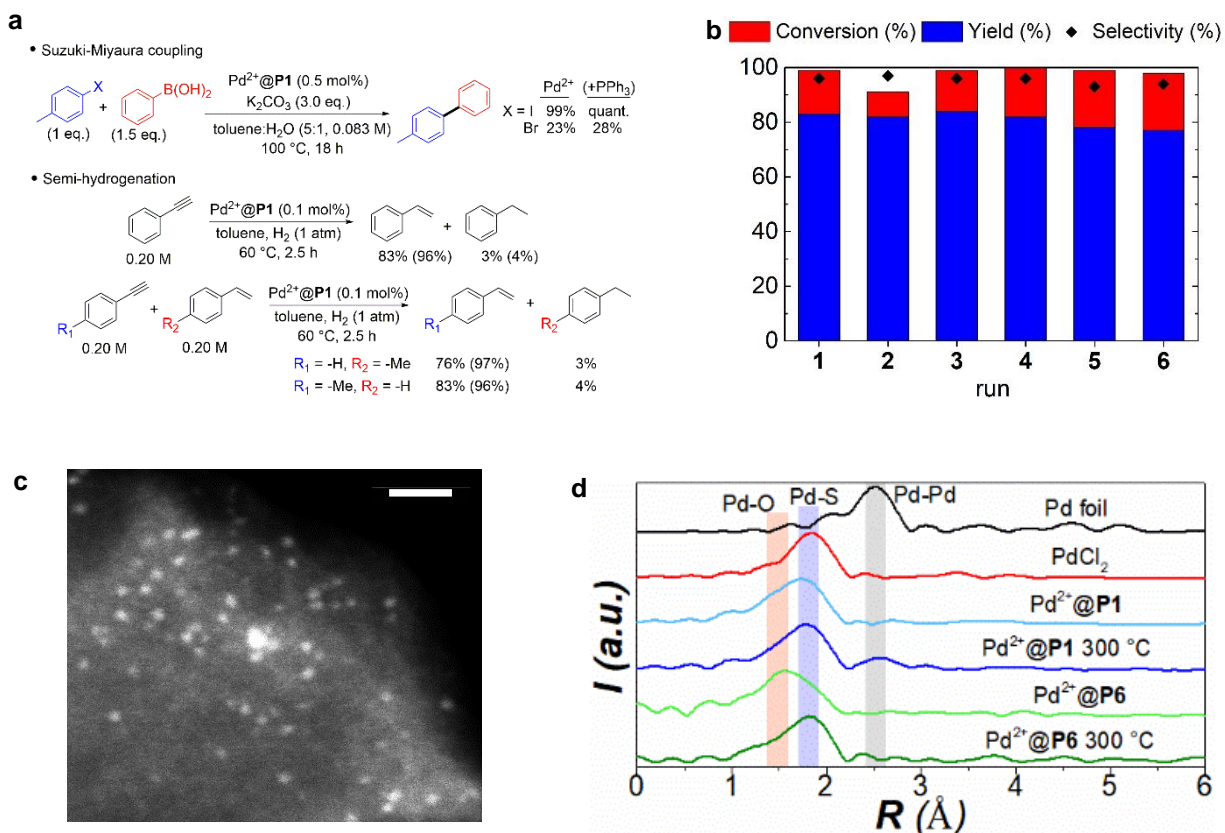


Figure 4. a Reactivity of the Pd²⁺@P1 (1 wt% Pd) framework as heterogeneous catalyst. Yields are shown and values in parentheses stand for selectivity of semi- vs. complete hydrogenation. **b** Reusability of Pd²⁺@P1 over 6 cycles of phenylacetylene semi-hydrogenation. **c** HAADF image of Pd²⁺@P1 after Suzuki reaction (bar represents 10 nm). **d** k²-weighted Fourier transform of the EXAFS function for Pd²⁺@P1 and Pd²⁺@P6 at RT and 300 °C under H₂ stream and selected references. Pd-O interaction is due to the hydration of the Pd²⁺.

CONCLUSIONS AND OUTLOOK

As a summary, we have developed a new methodology to synthesise previously unknown porous polymers linked by strong thioether bonds, which are difficult to access by traditional synthetic methods, by using the reversible Pd-catalysed C–S/C–S metathesis reaction. The materials are obtained in good yields, with high surface areas and are extremely resistant against several harsh conditions including aggressive chemicals. We have demonstrated the importance of the reaction's reversibility in order to produce high quality frameworks and good control over their properties. Importantly, the polymers have been designed to be recycled after use by degrading them back to the monomers using palladium catalysis. This design concept is highly relevant in the context of circular economy. In addition, the frameworks could be applied in different environmentally relevant fields: metal capture, metal sensing and heterogeneous catalysis, both in liquid and gas phase. In particular, P4 outperforms previously reported materials in Pd²⁺ sensing, detecting down to 2 ppb with great selectivity. Besides these exciting preliminary results, given the novelty of this family of materials, we believe that many more applications can be developed in different fields such as photo/electrocatalysis or gas capture. In a broader context, we believe this work demonstrates the untapped potential of emerging single-bond metathesis reactions in the area of materials science.

Methods

All reactions were carried out under argon in oven-dried glassware using anhydrous solvents. All commercially available compounds were used as received from common suppliers (Sigma-Aldrich, Strem Chemicals, Abcr, TCI, Fluorochem, Acros Organics, Alfa Aesar and Apollo Scientific).

NMR spectra were recorded on Bruker AVANCE III 400, Neo 400, Neo 500, or 600 spectrometers at room temperature; the chemical shifts are reported with respect to internal solvent: $\delta\text{H} = 7.26$ ppm, and $\delta\text{C} = 77.16$ (t) ppm (CDCl₃); $\delta\text{H} = 7.16$ ppm, and $\delta\text{C} = 128.06$ (t) ppm (C₆D₆); $\delta\text{H} = 2.50$ (p) ppm, and $\delta\text{C} = 39.52$ (hept) ppm (DMSO-d₆). Multiplicities are indicated by s (singlet), d (doublet), t (triplet), q (quartet), p (quintet), h (sextet), hept (septet),

m(multiplet), br (broad), or combinations thereof. GC/FID were measured in a Shimadzu GC-2025 (capillary column: Macherey-Nagel OPTIMA 5, 30.0 m × 0.25 mm × 0.25 μm; carrier gas: H₂); To determine GC yields, calibration curves were generated using *n*-dodecane as an internal standard.

High-resolution MS (HRMS) were acquired with a Thermo scientific Q-Exactive GC Orbitrap for EI. Bruker Daltonics maXis ESI-QTOF or solariX ESI-FTICR-MS for ESI. Elemental analysis (EA): C, H, and N measurements were performed in a LECO TruSpec Micro instrument. The gaseous combustion products of C (CO₂) and H (H₂O) were quantified by means of infrared spectroscopy. Nitrogen was measured as N₂ with a thermal conductivity detector. Sulphur was measured in a HEKAtech EuroVector instrument by burning the sample at 1000 °C with an excess of O₂. The composition products were chromatographically separated and measured with a thermal conductivity detector. HRMS and EA were performed in the Molecular and Biomolecular Analysis Service (MoBiAS) in the Laboratorium für Organische Chemie at ETH Zürich. Elemental analyses of Pd and Au for all materials were performed by Inductively Coupled Plasma-Optical Emission Spectrometry (ICP-OES) by the Mikroanalytisches Labor Pascher, Remagen.

Transmission Electron Microscopy (TEM): The morphology of the samples, as well as metal distribution and metal particle sizes were obtained by high resolution TEM using a FEI Talos F200X instrument. The samples were prepared by dropcasting a dispersion of the polymers on a copper grid coated with carbon film. Scanning Electron Microscopy (SEM): The morphology and particle sizes of the polymers were analysed by field emission scanning electron microscopy (FE-SEM) using a JEOL JSM-7100F instrument. The samples were prepared by dropcasting a dispersion of the polymers on a copper tape film and coated with carbon using a CCU-010 Carbon Coater Safematic instrument.

N₂ physisorption: The specific surface area of the materials and the porosity were measured from a nitrogen physisorption isotherm recorded at -196 °C on a BEL JAPAN BELSORP-min apparatus. The surface area values were obtained by the BET method. The pore sizes were obtained by the BJH method using the adsorption branch. The samples were dried at 60 °C under N₂ flow for 16 hours and then 2 hours under vacuum at 100 °C.

X-ray Absorption Spectroscopy (XAS): was conducted at the SuperXAS beamline of the Swiss Light Source (proposal number 20200442). The X-ray beam from the 2.9 T superbend was collimated using a Pt-coated mirror, monochromatised using a Si(111) channel cut monochromator, and focused to a spot size of 500×100 μm (horizontal×vertical) using a Pt-coated toroidal mirror. Data were acquired in air from pressed pellets at the Pd K-edge in transmission and fluorescence modes simultaneously using Quick XAS data acquisition mode, using three 15 cm long Ar/N₂-filled ionization chambers for transmission detection and PIPs diode for fluorescence detection. The samples were placed between the first and the second ionisation chamber. For the absolute energy calibration, a Pd foil was

measured simultaneously between the second and a third ionisation chambers. The resulting data were averaged and energy calibrated using ProXAS in house software and background corrected and normalised using the Athena program from the Demeter software suite. Fourier transformation of EXAFS data was performed using k^2 weightings in the range of 3-12 \AA^{-1} .

Fourier Transformed Infrared spectroscopy (FT-IR) measurements were carried out using a Bruker INVENIO-R FT-IR Spectrometer equipped with a diamond ATR crystal. Ultraviolet-visible (UV-vis) measurements of the polymers were carried out in a dispersion of dichloromethane using a quartz cuvette in a Cary 60 UV-Vis spectrophotometer. Fluorescence quenching experiments as well as fluorescence spectra of the polymers were performed in an aqueous dispersion (1% v/v NMP) using a Tecan Infinite 200 PRO plate reader.

Author Contributions

B.M. and M.A.R.-C. conceived the project and wrote the manuscript, M.A.R.-C. performed the mechanistic studies, synthesis and of the frameworks and their applications, M.A.R.-C. and G.T. carried out the application of the materials in heterogeneous catalysis, all authors contributed to the manuscript and SI.

ACKNOWLEDGMENTS

The authors thank ETH and the European Research Council under the European Union's Horizon 2020 research and innovation program (Shuttle Cat, Project ID: 757608) for funding. M.A.R.-C. thanks Fundación Ramón Areces for a fellowship. G.T. thanks Studienstiftung des deutschen Volkes for a fellowship. ScopeM, SMOOC and Prof. Copéret are acknowledged for providing access to electron microscopy, powder XRD and N_2 physisorption instruments, respectively. We thank Dr. Olga Safonova (PSI) for her technical assistance in the XAS experiments. Ori Green, Marius Lutz and Michael Bogdos from Prof. Morandi's group are acknowledged for their help in XAS measurements.

REFERENCES

- 1 Feng, X., Ding, X. & Jiang, D. Covalent organic frameworks. *Chemical Society Reviews* **41**, 6010-6022, doi:10.1039/c2cs35157a (2012).
- 2 Ding, S. Y. & Wang, W. Covalent organic frameworks (COFs): from design to applications. *Chem. Soc. Rev.* **42**, 548-568, doi:10.1039/c2cs35072f (2013).
- 3 Segura, J. L., Mancheno, M. J. & Zamora, F. Covalent organic frameworks based on Schiff-base chemistry: synthesis, properties and potential applications. *Chem. Soc. Rev.* **45**, 5635-5671, doi:10.1039/c5cs00878f (2016).
- 4 Zhu, L. & Zhang, Y. B. Crystallization of Covalent Organic Frameworks for Gas Storage Applications. *Molecules* **22**, doi:10.3390/molecules22071149 (2017).

- 5 Wang, J. & Zhuang, S. Covalent organic frameworks (COFs) for environmental applications. *Coord. Chem. Rev.* **400**, doi:10.1016/j.ccr.2019.213046 (2019).
- 6 Zhao, X. *et al.* Macro/Microporous Covalent Organic Frameworks for Efficient Electrocatalysis. *J. Am. Chem. Soc.* **141**, 6623-6630, doi:10.1021/jacs.9b01226 (2019).
- 7 Rodriguez-San-Miguel, D. & Zamora, F. Processing of covalent organic frameworks: an ingredient for a material to succeed. *Chem. Soc. Rev.* **48**, 4375-4386, doi:10.1039/c9cs00258h (2019).
- 8 Wang, Z., Zhang, S., Chen, Y., Zhang, Z. & Ma, S. Covalent organic frameworks for separation applications. *Chem. Soc. Rev.* **49**, 708-735, doi:10.1039/c9cs00827f (2020).
- 9 Geng, K. *et al.* Covalent Organic Frameworks: Design, Synthesis, and Functions. *Chem. Rev.*, doi:10.1021/acs.chemrev.9b00550 (2020).
- 10 Kaur, P., Hupp, J. T. & Nguyen, S. T. Porous Organic Polymers in Catalysis: Opportunities and Challenges. *ACS Catal.* **1**, 819-835, doi:10.1021/cs200131g (2011).
- 11 Byun, Y., Je, S. H., Talapaneni, S. N. & Coskun, A. Advances in Porous Organic Polymers for Efficient Water Capture. *Chem. Eur. J.* **25**, 10262-10283, doi:10.1002/chem.201900940 (2019).
- 12 Díaz, U. & Corma, A. Ordered covalent organic frameworks, COFs and PAFs. From preparation to application. *Coord. Chem. Rev.* **311**, 85-124, doi:10.1016/j.ccr.2015.12.010 (2016).
- 13 Lee, J. M. & Cooper, A. I. Advances in Conjugated Microporous Polymers. *Chem. Rev.* **120**, 2171-2214, doi:10.1021/acs.chemrev.9b00399 (2020).
- 14 Wang, W. & Schlüter, A. D. Synthetic 2D Polymers: A Critical Perspective and a Look into the Future. *Macromol. Rapid Commun.* **40**, 1800719, doi:10.1002/marc.201800719 (2019).
- 15 Jin, Y., Wang, Q., Taynton, P. & Zhang, W. Dynamic covalent chemistry approaches toward macrocycles, molecular cages, and polymers. *Acc. Chem. Res.* **47**, 1575-1586, doi:10.1021/ar500037v (2014).
- 16 Rahate, A. S., Nemade, K. R. & Waghuley, S. A. Polyphenylene sulfide (PPS): state of the art and applications. *Rev. Chem. Eng.* **29**, doi:10.1515/revce-2012-0021 (2013).
- 17 Zuo, P., Tcharkhtchi, A., Shirinbayan, M., Fitoussi, J. & Bakir, F. Overall Investigation of Poly (Phenylene Sulfide) from Synthesis and Process to Applications—A Review. *Macromol. Mater. Eng.* **304**, 1800686, doi:10.1002/mame.201800686 (2019).
- 18 Horiuchi, S. *et al.* Well-Controlled Synthesis of Poly (phenylene sulfide) (PPS) Starting from Cyclic Oligomers. *Macromol. Symp.* **349**, 9-20, doi:10.1002/masy.201300221 (2015).
- 19 Van Bierbeek, A. & Gingras, M. Polysulfurated branched molecules containing functionalized m-phenylene sulfides. *Tetrahedron Letters* **39**, 6283-6286, doi:https://doi.org/10.1016/S0040-4039(98)01327-6 (1998).
- 20 Cao, Y. *et al.* Porous Organic Polymers Containing a Sulfur Skeleton for Visible Light Degradation of Organic Dyes. *Chem Asian J* **14**, 2883-2888, doi:10.1002/asia.201900477 (2019).
- 21 Ong, W. J. & Swager, T. M. Dynamic self-correcting nucleophilic aromatic substitution. *Nat. Chem.* **10**, 1023-1030, doi:10.1038/s41557-018-0122-8 (2018).

- 22 Lian, Z., Bhawal, B. N., Yu, P. & Morandi, B. Palladium-catalyzed carbon-sulfur or carbon-phosphorus bond metathesis by reversible arylation. *Science* **356**, 1059-1063, doi:10.1126/science.aam9041 (2017).
- 23 Delcaillau, T., Bismuto, A., Lian, Z. & Morandi, B. Nickel-Catalyzed Inter- and Intramolecular Aryl Thioether Metathesis by Reversible Arylation. *Angew. Chem. Int. Ed.* **59**, 2110-2114, doi:10.1002/anie.201910436 (2020).
- 24 Chen, Y., Abdellatif, M. M. & Nomura, K. Olefin metathesis polymerization: Some recent developments in the precise polymerizations for synthesis of advanced materials (by ROMP, ADMET). *Tetrahedron* **74**, 619-643, doi:https://doi.org/10.1016/j.tet.2017.12.041 (2018).
- 25 Sutthasupa, S., Shiotsuki, M. & Sanda, F. Recent advances in ring-opening metathesis polymerization, and application to synthesis of functional materials. *Polym. J.* **42**, 905-915, doi:10.1038/pj.2010.94 (2010).
- 26 Matsumoto, M. *et al.* Rapid, Low Temperature Formation of Imine-Linked Covalent Organic Frameworks Catalyzed by Metal Triflates. *J. Am. Chem. Soc.* **139**, 4999-5002, doi:10.1021/jacs.7b01240 (2017).
- 27 Zhu, Y., Yang, H., Jin, Y. & Zhang, W. Porous Poly(aryleneethynylene) Networks through Alkyne Metathesis. *Chem. Mater.* **25**, 3718-3723, doi:10.1021/cm402090k (2013).
- 28 Yang, H. *et al.* Aromatic-rich hydrocarbon porous networks through alkyne metathesis. *Mater. Chem. Front.* **1**, 1369-1372, doi:10.1039/c6qm00359a (2017).
- 29 Feriante, C. H. *et al.* Rapid Synthesis of High Surface Area Imine-Linked 2D Covalent Organic Frameworks by Avoiding Pore Collapse During Isolation. *Adv. Mater.* **32**, e1905776, doi:10.1002/adma.201905776 (2020).
- 30 Smith, B. J. *et al.* Colloidal Covalent Organic Frameworks. *ACS Cent. Sci.* **3**, 58-65, doi:10.1021/acscentsci.6b00331 (2017).
- 31 Beck, H. N. Process for forming articles comprising poly(phenylene sulfide) (PPS), US5043112 (Dow Chemical Co, 1991).
- 32 Sherwood, J., Clark, J. H., Fairlamb, I. J. S. & Slatery, J. M. Solvent effects in palladium catalysed cross-coupling reactions. *Green Chem.* **21**, 2164-2213, doi:10.1039/C9GC00617F (2019).
- 33 Molina de la Torre, J. A., Espinet, P. & Albéniz, A. C. Solvent-Induced Reduction of Palladium-Aryls, a Potential Interference in Pd Catalysis. *Organometallics* **32**, 5428-5434, doi:10.1021/om400713y (2013).
- 34 Flahive, E. *et al.* A High-Throughput Methodology for Screening Solution-Based Chelating Agents for Efficient Palladium Removal. *QSAR Comb. Sci.* **26**, 679-685, doi:10.1002/qsar.200610124 (2007).
- 35 Guan, X. *et al.* Chemically stable polyarylether-based covalent organic frameworks. *Nat. Chem.* **11**, 587-594, doi:10.1038/s41557-019-0238-5 (2019).
- 36 Ravindra, K., Bencs, L. & Van Grieken, R. Platinum group elements in the environment and their health risk. *Sci. Total Environ.* **318**, 1-43, doi:https://doi.org/10.1016/S0048-9697(03)00372-3 (2004).
- 37 Yang, P., Shu, Y., Zhuang, Q., Li, Y. & Gu, J. A robust MOF-based trap with high-density active alkyl thiol for the super-efficient capture of mercury. *Chem. Commun.* **55**, 12972-12975, doi:10.1039/c9cc06255f (2019).
- 38 Huang, N., Zhai, L., Xu, H. & Jiang, D. Stable Covalent Organic Frameworks for Exceptional Mercury Removal from Aqueous Solutions. *J. Am. Chem. Soc.* **139**, 2428-2434, doi:10.1021/jacs.6b12328 (2017).
- 39 Hong, Y. *et al.* Precious metal recovery from electronic waste by a porous porphyrin polymer. *Proc. Natl. Acad. Sci. U.S.A.* **117**, 16174-16180, doi:10.1073/pnas.2000606117 (2020).

- 40 Bowron, D. T., Beret, E. C., Martin-Zamora, E., Soper, A. K. & Sánchez Marcos, E. Axial Structure of the Pd(II) Aqua Ion in Solution. *J. Am. Chem. Soc.* **134**, 962-967, doi:10.1021/ja206422w (2012).
- 41 Li, H., Fan, J. & Peng, X. Colourimetric and fluorescent probes for the optical detection of palladium ions. *Chem. Soc. Rev.* **42**, 7943-7962, doi:10.1039/C3CS60123D (2013).
- 42 Wang, M., Yuan, Y., Wang, H. & Qin, Z. A fluorescent and colorimetric probe containing oxime-ether for Pd²⁺ in pure water and living cells. *Analyst* **141**, 832-835, doi:10.1039/C5AN02225H (2016).
- 43 Duan, L., Xu, Y. & Qian, X. Highly sensitive and selective Pd²⁺ sensor of naphthalimide derivative based on complexation with alkynes and thio-heterocycle. *Chem. Commun.*, 6339-6341, doi:10.1039/B815298E (2008).
- 44 Liu, B. *et al.* Synthesis and characterization of a fluorescent polymer containing 2,6-bis(2-thienyl)pyridine moieties as a highly efficient sensor for Pd²⁺ detection. *Chem. Commun.* **47**, 1731-1733, doi:10.1039/C0CC03819A (2011).
- 45 Helal, A., Nguyen, H. L., Al-Ahmed, A., Cordova, K. E. & Yamani, Z. H. An Ultrasensitive and Selective Metal–Organic Framework Chemosensor for Palladium Detection in Water. *Inorg. Chem.* **58**, 1738-1741, doi:10.1021/acs.inorgchem.8b02871 (2019).
- 46 Vile, G. *et al.* A stable single-site palladium catalyst for hydrogenations. *Angew. Chem. Int. Ed. Engl.* **54**, 11265-11269, doi:10.1002/anie.201505073 (2015).
- 47 Chen, Z. *et al.* A heterogeneous single-atom palladium catalyst surpassing homogeneous systems for Suzuki coupling. *Nat. Nanotechnol.* **13**, 702-707, doi:10.1038/s41565-018-0167-2 (2018).
- 48 Lee, S. *et al.* Dynamic metal-polymer interaction for the design of chemoselective and long-lived hydrogenation catalysts. *Sci. Adv.* **6**, eabb7369, doi:10.1126/sciadv.abb7369 (2020).
- 49 Albani, D. *et al.* Selective ensembles in supported palladium sulfide nanoparticles for alkyne semi-hydrogenation. *Nat. Commun.* **9**, 2634, doi:10.1038/s41467-018-05052-4 (2018).
- 50 Huang, X. *et al.* Toward Understanding of the Support Effect on Pd¹ Single-Atom-Catalyzed Hydrogenation Reactions. *The Journal of Physical Chemistry C* **123**, 7922-7930, doi:10.1021/acs.jpcc.8b07181 (2019).